Ultramicroscopy 111 (2011) 877–886

Contents lists available at ScienceDirect

Ultramicroscopy

journal homepage: www.elsevier.com/locate/ultramic

Bright-field scanning confocal electron microscopy using a double aberration-corrected transmission electron microscope

Peng Wang [a], Gavin Behan [a,1], Angus I. Kirkland [a], Peter D. Nellist [a,*], Eireann C. Cosgriff [b], Adrian J. D'Alfonso [b], Andrew J. Morgan [b], Leslie J. Allen [b], Ayako Hashimoto [c], Masaki Takeguchi [c,d], Kazutaka Mitsuishi [c,e], Masayuki Shimojo [d,f]

[a] Department of Materials, University of Oxford, Parks Road, Oxford OX1 3PH, UK
[b] School of Physics, University of Melbourne, Parkville, Victoria 3010, Australia
[c] Advanced Nano-characterization Center, National Institute for Materials Science (NIMS), 3-13 Sakura, Tsukuba 305-0003, Japan
[d] High Voltage Electron Microscopy Station, NIMS, 3-13 Sakura, Tsukuba 305-0003, Japan
[e] Quantum Dot Research Center, NIMS, 3-13 Sakura, Tsukuba 305-0003, Japan
[f] Advanced Science Research Laboratory, Saitama Institute of Technology, 1690 Fusaiji, Fukaya 369-0293, Japan

ARTICLE INFO

Available online 27 October 2010

Keywords:
Three dimensional
Confocal
SCEM
Aberration-correction

ABSTRACT

Scanning confocal electron microscopy (SCEM) offers a mechanism for three-dimensional imaging of materials, which makes use of the reduced depth of field in an aberration-corrected transmission electron microscope. The simplest configuration of SCEM is the bright-field mode. In this paper we present experimental data and simulations showing the form of bright-field SCEM images. We show that the depth dependence of the three-dimensional image can be explained in terms of two-dimensional images formed in the detector plane. For a crystalline sample, this so-called probe image is shown to be similar to a conventional diffraction pattern. Experimental results and simulations show how the diffracted probes in this image are elongated in thicker crystals and the use of this elongation to estimate sample thickness is explored.

1. Introduction

Confocal scanning optical microscopy (CSOM) is an established technique in light optics [1]. The basis of the technique is the restriction of contributions to the image from scattering occurring at points not in the confocal plane. Making use of the restricted depth of field of optics with a large numerical aperture and preferentially weighting the scattering at the confocal plane leads to the so-called optical sectioning effect. Such an approach leads to a greater depth resolution and selectivity than that of the wide-field microscope and allows three-dimensional (3-D) information to be retrieved by recording images over a series of focal plane depths.

Using transmission electron microscopy (TEM), Frigo et al. [2] have shown improved image contrast in very thick specimens using a scanning confocal configuration. The depth of field is inversely proportional to the square of the numerical aperture of the objective lens [1,3] and the relatively low numerical aperture used in the experiments of Frigo et al. [2], imposed by the inherent spherical aberration of the lenses [4], did not allow depth information to be retrieved. Nonetheless, improved lateral resolution in very thick samples was demonstrated.

The development of spherical aberration correctors for both TEM and scanning transmission electron microscopy (STEM) has dramatically improved the lateral resolution of 2-D images [5]. The larger numerical aperture available also reduces the depth of field to typically just a few nanometres, which suggests that a confocal imaging mode using electrons may be a promising technique for 3-D imaging at the nanometre scale.

Nellist et al. [6] have shown that a TEM/STEM instrument fitted with two aberration correctors can be aligned in a confocal mode. Using this mode of imaging in a 200 kV instrument with 30 mrad semi-angle apertures in both the pre- and post-specimen lenses gives a predicted depth resolution of 3.5 nm. The simplest detectable SCEM signal is the intensity of electrons that pass through the small detector-plane collector aperture, a technique referred to subsequently in this paper as bright-field (BF) SCEM. The electron optical configuration for SCEM is shown in Fig. 1. In SCEM the pre-specimen optics are the same as for STEM, while the lower optics are used to focus electrons that have been scattered from the confocal point (a) (in Fig. 1) onto a collector aperture in the detector plane. Electrons scattered from elsewhere are focused to a point either above or below the point detector and so their contribution to the image intensity is reduced. The confocal point can subsequently be scanned in a

* Corresponding author.
E-mail address: peter.nellist@materials.ox.ac.uk (P.D. Nellist).
[1] Now at CRANN, Trinity College Dublin, Dublin 2, Ireland

0304-3991/$ - see front matter © 2010 Elsevier B.V. All rights reserved.
doi:10.1016/j.ultramic.2010.10.012

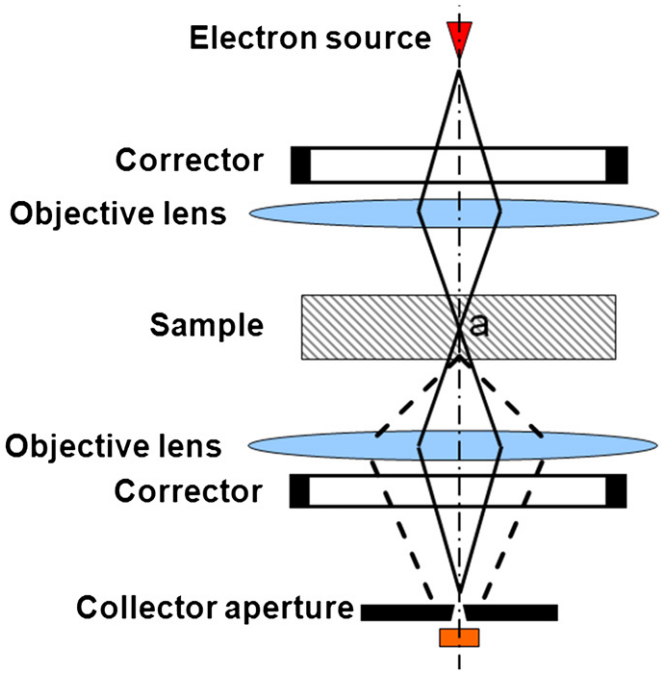

Fig. 1. Schematic diagram of ray paths for BFSCEM, showing beams (dashed line) scattered away from the confocal point, marked 'a', are rejected by the collector aperture.

three-dimensional raster to form a 3-D image. Alternatively 2-D slice images or 1-D line profiles along arbitrary orientations can be recorded. In addition to BFSCEM there are alternative SCEM modes, such as energy-filtered SCEM [7] and annular dark field SCEM [8,9], which are discussed elsewhere. Because SCEM is a new technique in electron microscopy, it is necessary to evaluate and compare the resolution limits, image contrast mechanisms and potential applications of the SCEM modes proposed. The simplest configuration is BFSCEM and this mode also offers the greatest efficiency in terms of the fraction of incident electrons detected. The purpose of this paper is to evaluate the BFSCEM mode.

Einspahr and Voyles [10] have previously considered the appropriate contrast transfer function (CTF) using the scalar-wave linear imaging theory adapted from light confocal microscopy. The linear imaging theory assumes that the scattering by the object is so weak that perturbation on the illuminating beam by the specimen is small. In the coherent linear imaging approximation, the SCEM image intensity can be expressed as follows [11]:

$$I(\mathbf{R}) = \left|\xi(\mathbf{R}) \otimes [\Phi_1(\mathbf{R})\Phi_2(\mathbf{R})]\right|^2, \quad (1)$$

where $\xi(\mathbf{R})$ is the transmission function of the specimen, Φ_1 and Φ_2 are the 3-D coherent point-spread functions of the pre- and post-specimen optics, respectively, and $\otimes$ denotes convolution over the 3-D position vector, $\mathbf{R}$. The point-spread function for coherent SCEM is therefore the product $\Phi_1(\mathbf{R})\Phi_2(\mathbf{R})$. The CTF is the 3-D Fourier transform of the confocal point-spread function, and Fig. 2 shows the CTF of BFSCEM calculated with the pre- and post-specimen apertures of 22 and 17.7 mrad, respectively, as used in the experiments described here. As discussed previously [12,13], the CTF describes the information transfer, which is possible for a given imaging mode and geometry. The missing cones of information transfer that are shown in Fig. 2 can lead to significant elongation in 3-D images. This elongation is dependent on the lateral extent of the object being imaged. The uneven bounds of the transfer function in Fig. 2 are a consequence of the different aperture sizes.

Cosgriff et al. [14] have shown that there is no linear, first-order transfer of contrast in weak-phase object approximation when

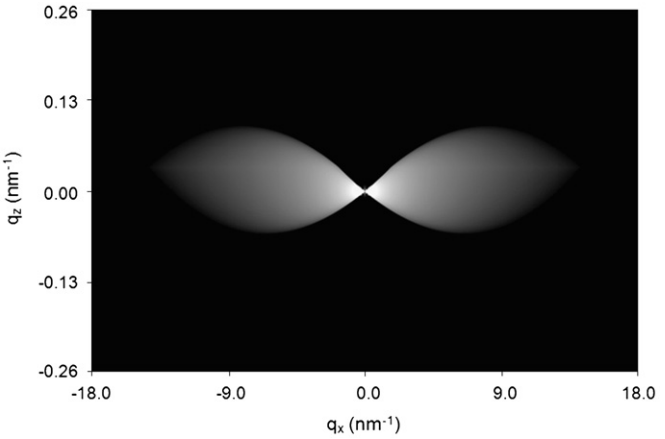

Fig. 2. Amplitude BFSCEM CTF calculated with pre- and post-specimen apertures of 22 and 17.7 mrad, respectively.

using BFSCEM. Contrast can therefore only arise from multiple elastic scattering. The effects of multiple elastic scattering are included in the dynamical theory of electron diffraction, and this is particularly important for thicker samples, or those comprising heavier elements. In dynamical diffraction, intensity can be transferred from one reflection to another as the wave propagates, altering the diffraction pattern's intensity distribution. This complicates the interpretation of electron scattering and in general dynamical effects have to be carefully considered when interpreting TEM data. For BFSCEM, Cosgriff et al. [14] theoretically calculated the image contrast from a zone-axis aligned GaAs crystalline sample using elastically scattered electrons. These calculations showed that dynamical scattering in the form of channelling plays an important role in the contrast mechanisms for thicker samples. Mitsuishi et al. have also showed the oscillatory behaviour of the BFSCEM image contrast as a function of the sample thickness using a Bloch wave image simulation method [15] and more recently using multislice simulations [16].

In this paper we compare BFSCEM data with simulation in order to explain the form of the contrast observed. Firstly we consider the images of the confocal plane theoretically and experimentally for a Si specimen placed some distance before the confocal plane. This observation allows us to explain the 'W'-shaped depth profile observed in experimental BFSCEM optical sectioning of an Au nanoparticle. We then return to the crystalline Si sample and explore how the data can reveal information about the crystal structure and thickness.

2. Imaging the confocal plane

All the experiments in this paper were performed using the Oxford-JEOL JEM 2200MCO fitted with spherical aberration correctors for both the pre- and post-specimen optics (an earlier version of the instrument is described in Ref. [17]). The confocal trajectory is established by following Ref. [6], as shown in Fig. 1. A Si ⟨1 1 0⟩ wedge sample was prepared by mechanical thinning, followed by ion milling. This sample gives a wide range of thicknesses depending on which part of the sample was used. The detector plane images, referred to as confocal plane images, were recorded on a 4k × 4k Gatan CCD camera with 2 × pixel binning and 4 s dwell time. The numerical apertures in the pre- and post-specimen optics were 22 and 17.7 mrad, respectively.

A typical image of the confocal plane is shown in Fig. 3(a) with the sample displaced from the confocal plane by 186 nm. Analogous to the diffraction pattern from a crystalline sample, the satellite diffracted probes in the confocal plane image in Fig. 3(a)